







Original Paper

Application of an improved TEM-EDS protocol based on charge balance for accurate chemical analysis of sub-micrometric phyllosilicates in low-grade metamorphic rocks

Edoardo Sanità¹ , Roberto Conconi² , Sofia Lorenzon¹ , Maria Di Rosa¹ , Giancarlo Capitani²  and Enrico Mugnaioli¹ 

¹Università di Pisa, Dipartimento di Scienze della Terra, Via Santa Maria, 53, Pisa, Italy and ²Università degli Studi di Milano-Bicocca, Dipartimento di Scienze dell'Ambiente e della Terra, Piazza della Scienza 4, Milano, Italy

Abstract

Determining the chemical composition of sub-micrometer rock-forming minerals is still a challenging task. The electron probe micro-analyzer (EPMA) is considered the most accurate analytical way to obtain chemical data on amorphous and crystalline materials. However, performing EPMA analyses on sub-micrometer-sized grains is uncertain not recommended as the risk of obtaining analyses contaminated from the surrounding phases. A transmission electron microscope (TEM) equipped with an energy dispersive X-ray spectrometer (EDS) provides a greater spatial resolution, making it possible to obtain trustworthy chemical information on sub-micrometer-sized material. In this work, we present a fast and cheap data-reduction protocol for TEM-EDS chemical analysis, where *k*-factors derived experimentally for each element of interest and absorption correction are implemented. The results are compared with those determined using standardless and non-corrected TEM-EDS protocols. The *k*-factor for oxygen plays a fundamental role and its value should be calculated from compounds similar to the phase of interest. For absorption correction, the contribution of hydrogen during structural formula recalculation is taken into account, like a lower net valence of oxygen. The robustness of this protocol was tested by performing TEM-EDS analyses on white mica grains from metapelites, belonging to the Internal Ligurian Units exposed in the Northern Apennines, the chemical composition of which is well constrained. Such a protocol has proven to provide high-quality results from both statistical and crystallo-chemical perspectives. Remarkably, the tested data-reduction protocol for TEM-EDS analysis provided chemical compositions consistent with the EPMA results previously obtained from the same samples.

Keywords: charge balance; EDS; metapelites; phyllosilicate; TEM

(Received: 04 June 2024; revised: 27 August 2024; accepted: 13 September 2024)

Introduction

Phyllosilicates are one of the main rock-forming mineral groups. Among them, white micas are common mineral constituents of sedimentary and metamorphic rocks, which represent most of the worldwide geological environments. White micas are also a reservoir for non-abundant and industrially relevant elements (e.g. Li; see Penniston-Dorland et al., 2012) and have thermobarometric applications for estimating pressure and temperature conditions experienced by rock volumes during metamorphism (e.g. Kübler, 1967; Massone and Schreyer, 1987; Guidotti and Sassi, 1998; Vidal and Parra, 2000; Battaglia, 2004; Dubacq et al., 2010; Kamzolkin et al., 2016). Most of these applications depend heavily on white mica chemistry, which can vary significantly in different geological settings.

EPMA, based on wavelength dispersive X-ray spectroscopy (WDS), is generally considered the most accurate method for chemical analysis of minerals using polished thin sections where the micro-texture of the original rock is preserved. During analysis set-up, an accurate calibration with standards of known composition is required, providing an analytical accuracy of ~1–2% for the major elements. Such accuracy makes EPMA an efficient tool for performing quantitative chemical investigations of rock-forming minerals. However, its application on sub-micrometer grains is not recommended, because of the relatively poor spatial resolution and the consequent high risk of chemical analyses becoming contaminated from the surroundings. This limitation raises issues for the chemical characterization of fine-grained minerals, such as typical white micas associated with low-grade metamorphism.

A TEM equipped with an EDS detector provides much greater spatial resolution than EPMA and can easily perform chemical analyses of single sub-micrometer mineral grains (e.g. Wunderlich et al., 1993; Stadelmann et al., 1995; Abad et al., 2006; Tarantola et al., 2009; Bourdelle et al., 2012). However, TEM-EDS data are generally considered to be semi-quantitative, with errors up to a few points in

Corresponding author: Edoardo Sanità; Email: edoardo.sanita@dst.unipi.it

Cite this article: Sanità E., Conconi R., Lorenzon S., Di Rosa M., Capitani G., & Mugnaioli E. (2024). Application of an improved TEM-EDS protocol based on charge balance for accurate chemical analysis of sub-micrometric phyllosilicates in low-grade metamorphic rocks. *Clays and Clay Minerals* 72, e31, 1–11. <https://doi.org/10.1017/cmn.2024.32>

weight percentage (wt.%). TEM-EDS accuracy can be improved by adopting reproducible experimental protocols, but chemical quantification is unavoidably affected by X-ray absorption within the sample. Several TEM-EDS packages offer various options that aim to improve the accuracy of the chemical analyses, taking into account the sample thickness and the matrix effects. However, these corrections are often neglected, because TEM-EDS data are considered qualitative, and therefore many laboratories do not calibrate their apparatus with standards of known composition.

In general, sample preparation for TEM-EDS may be more complicated and expensive than sample preparation for EPMA. The simplest protocol consists of grinding the sample in an agate mortar to obtain fine-grained particles, which can be easily dispersed onto a TEM grid, losing the original texture of the rock (e.g. Tarantola et al., 2009). Sample preparations by ion-milling or focus-ion beam (FIB) provide ultra-thin slices, where the original textural relationships are preserved (e.g. Bourdelle et al., 2012). However, ion-milling is a time-consuming procedure that does not guarantee the accurate location of the thinned area within the micro-textural site of interest. FIB appears to be a valid protocol for sample preparation for its ability to target with high precision the area of interest (Wirth, 2004; Benzerara et al., 2005; Obst et al., 2005), but is relatively more expensive and in certain cases can introduce artifacts due to chemical and structural damage or to the thickness variation along the thinned lamellae produced (Bourdelle et al., 2012).

Bourdelle et al. (2012) proposed a strategy to quantitatively investigate the chemical composition of chlorites using FIB-prepared samples. These authors developed a correction procedure to minimize artifact-related errors due to sample preparation, variation in thickness, and X-ray absorption. More recently, Conconi et al. (2023) compared three different methods for the general quantification of TEM-EDS analyses, namely the standardless method (STL) (Newbury et al., 1995; Newbury, 1998), the Cliff–Lorimer approximation (Cliff and Lorimer, 1975) and the absorption correction method (ACM) based on electroneutrality (van Cappellen and Doukhan, 1994). These authors highlighted the better performance of ACM compared with other data-reduction protocols for phases that contain heavy elements. However, for both Cliff–Lorimer approximation and ACM, the experimental calculation of accurate *k*-factors from standards of known composition is required.

In this paper, the ACM proposed by van Cappellen and Doukhan (1994) is applied for the quantitative chemical analysis by TEM-EDS of sub-micrometer white mica crystals from low-metamorphic pelites of the Palombini Shale Formation, which belongs to the Internal Ligurian Units (Northern Apennines; see Sanità et al., 2024 and references therein). The results are compared with those obtained by the STL method, by a calibrated but non-corrected (NC) TEM-EDS analysis and by EPMA. This preliminary application focuses only on the accuracy and robustness of a dataset of chemical analyses collected from single grains obtained by crushed samples, considering experimentally calibrated *k*-factor and the net valence correction of oxygen.

Materials and methods

Materials, sampling criteria, and preparation

Sampling area

The samples investigated in this study were collected on the Palombini Shale Formation, which belongs to the Internal Ligurian Units (Northern Apennines; Fig. 1). The Internal Ligurian Units sequence consists of sedimentary cover rocks ranging from Middle Jurassic to Paleogene, which overlay onto

an ophiolitic basement of Middle Jurassic age (e.g. Marroni et al., 2010; Marroni et al., 2017 and references therein for an exhaustive overview). The sedimentary cover is mostly represented by shales and arenites, and to a lesser extent by limestones and radiolarites. Recently, Meneghini et al. (2023) and Sanità et al. (2024) constrained the peak metamorphic conditions recorded by the Internal Ligurian Units using metapelites collected from the Palombini Shale Formation, providing reliable pressure and temperature conditions. The same samples analyzed by Meneghini et al. (2023) and Sanità et al. (2024) with EPMA have been used for the TEM-EDS analysis presented in this work.

Sampling criteria and petrographic observations

Four samples of carbonate-free metapelites (samples: ULI3bT, ULI8T, ULI14T, and ULI22aT; the final ‘T’ indicates samples used in the TEM-EDS analysis) were collected from tectonic units where the presence of the Palombini Shale Formation is documented (Fig. 1). All samples are characterized by a pervasive syn-metamorphic tectonic foliation developed during the under-thrusting and the subsequent accretion into the Alpine wedge (Fig. 2a,b; cf. S1 foliation of Meneghini et al., 2023 and Sanità et al., 2024). The latter foliation is usually characterized by a chlorite (Chl) + white mica (Wm) + quartz (Qz) ± albite (Ab) and ± calcite (Cc) mineral assemblage (Marroni and Pandolfi, 1996; Meneghini et al., 2023; Sanità et al., 2024), but detrital phyllosilicates and feldspars were also observed (mineral abbreviations after Warr, 2021). The detrital grains reach up to 50–60 µm in size (Fig. 2b), while the syn-metamorphic ones are smaller and never exceed 15 µm. In particular, micro-domains characterized by very fine-grained (a few micrometers in size) Wm and Chl crystals have been detected along the syn-metamorphic foliation (Fig. 2b). Syn-metamorphic Chl and Wm growing along the S1 foliation show sharp edges, with no evidence of chemical zoning (Meneghini et al., 2023; Sanità et al., 2024).

Sample preparation procedure

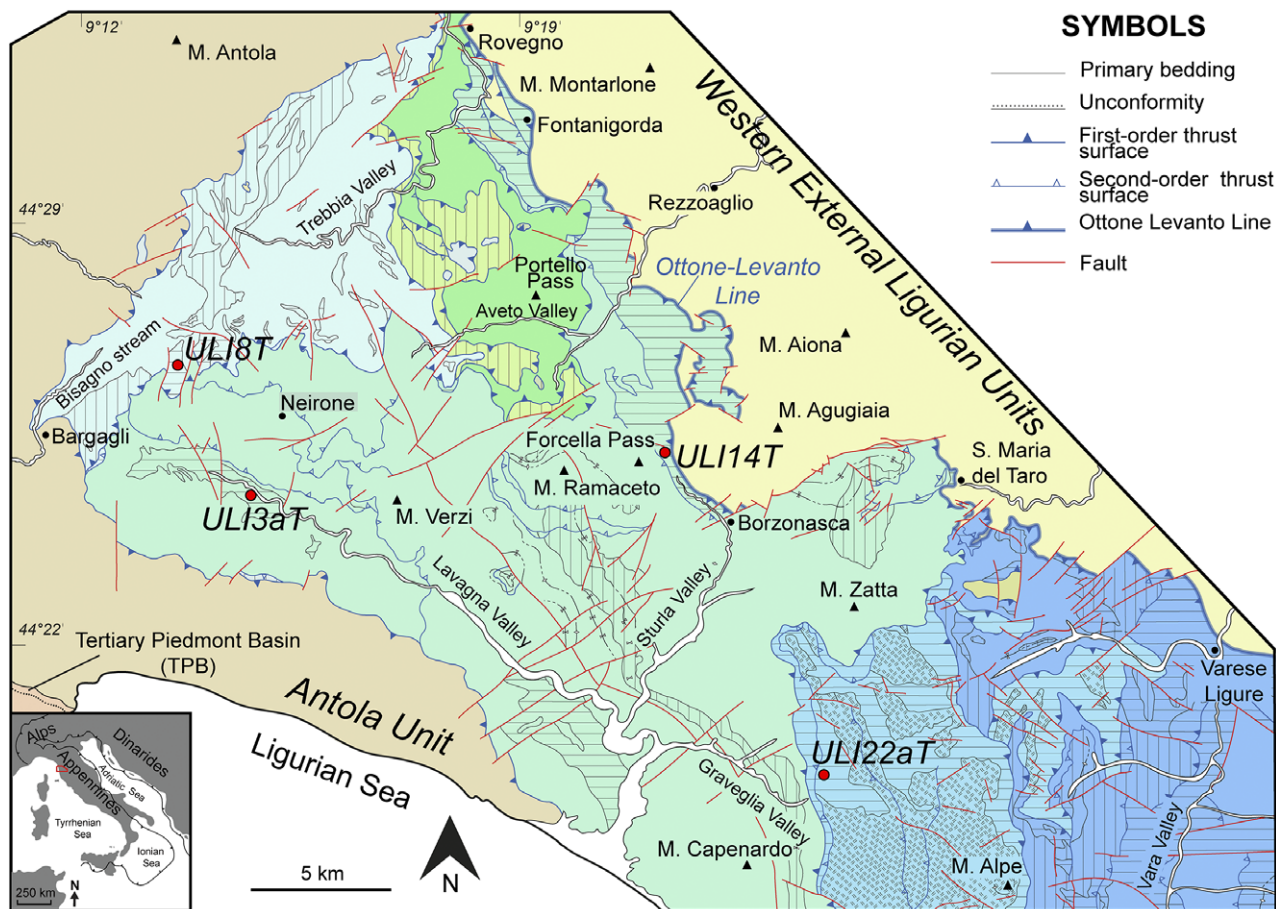
The Wm grains grown along the S1 foliation are the focus of this paper and a careful preparation protocol was adopted to obtain samples almost free from (usually larger) detrital phyllosilicates. Fresh, carbonate-poor metapelites, where S1 is preserved, were disaggregated in a jaw crusher for ~20 min, to obtain the whole-rock powders following the procedure proposed by Leoni et al. (1996). The whole-rock powders were subsequently treated to separate the <2 µm particles via differential settling for 4 h with distilled water. Subsequently, the natant was separated by the aqueous suspension using the water-bath, for at least 12 h. After that, the residual <2 µm powders were treated with ethanol and pipetted onto TEM Cu-grids covered by a film of amorphous graphite.

Such preparation is aimed to increase the concentration of syn-metamorphic Wm crystals in the powdered sample (Lezzerini et al., 1995; Leoni et al., 1996). Besides, because of their habit and crystallographic features, Wm (or phyllosilicates, *sensu lato*) grains will tend to lay with the (001) facet parallel to the grid surface, minimizing their projected thickness.

Acquisition settings and adopted corrections

TEM-EDS data acquisition and reduction

A multipurpose JEOL JEM-F200 TEM, working at 200 kV and equipped with a Schottky FEG source and a windowless silicon drift detector with an effective area of 100 mm², was used for TEM-EDS analyses. Data acquisition and analysis were performed with the JEOL Analysis Station software included in the TEM-EDS device.



LEGEND

External Ligurian Domain

Antola Unit

Undifferentiated

Western Ligurian Units

Undifferentiated

Internal Ligurian Domain

Portello Unit

Monte Lavagnola Formation - (Paleocene?)
Ronco Formation - (early Campanian)
Palombini Shale - (Santoniano-early Campanian)

Vermallo Unit

Cassingheno Formation - FCS (early Paleocene?)

Due Ponti Unit

Canale Formation - (Santonian-early Campanian)

Gottero Unit

Bocco Shale - (early Paleocene)
Gottero Sandstone - and Val Lavagna Group - (early Campanian-early Paleocene)
Palombini Shale - (Aptian-Santonian)

Bracco-Val Graveglia Unit

Palombini Shale (Berriasian-Albian) -
Ophiolite sequence - Oph (Middle to Late Jurassic), Cherts - DSD and Calpionella Limestone - CL (Callovian-Valanginian)

Colli-Tavarone Unit

Tavarone Formation - FCT (early Paleocene)
Val Lavagna Group - SVL (early Campanian-early Maastrichtian)
Palombini Shale - PBS (Berriasian-Albian)

Figure 1. Geological map of the sampled area (modified from Sanità et al., 2024) in which the Internal Ligurian Units are shown with different colors. The locations of the samples used in this work are indicated by red points.

All acquisitions were performed in scanning transmission electron microscopy (STEM) mode with an emission current of 77.78 A, a 40 μm CL aperture, a probe size of 6, an acquisition area of $\sim 50 \text{ nm}^2$, and a time of 60 s. The sample was tilted 15° around the x -axis (tilt- X) to maximize the EDS gain. The counts per second (cps) ranged between 4000 and 15,000, with a death time never higher than 30%.

EDS data reduction was performed following three different procedures, as explained in the next two paragraphs. During

quantifications, both the wt.% (SiO_2 , Al_2O_3 , TiO_2 , MnO , Cr_2O_3 , MgO , FeO , CaO , K_2O , and Na_2O) and the equivalent atomic percentage (at.%) of pure elements (O, Si, Al, Ti, Mn, Cr, Mg, Fe, Ca, K, and Na) were calculated (see [Supplementary material SI-S1, -S2 and -S3](#)). This choice is for two reasons: (1) the elemental at.% of pure elements promotes a fast quality check of newly measured k -factors and an easy calculation of cation and anion curves, used to determine the thickness

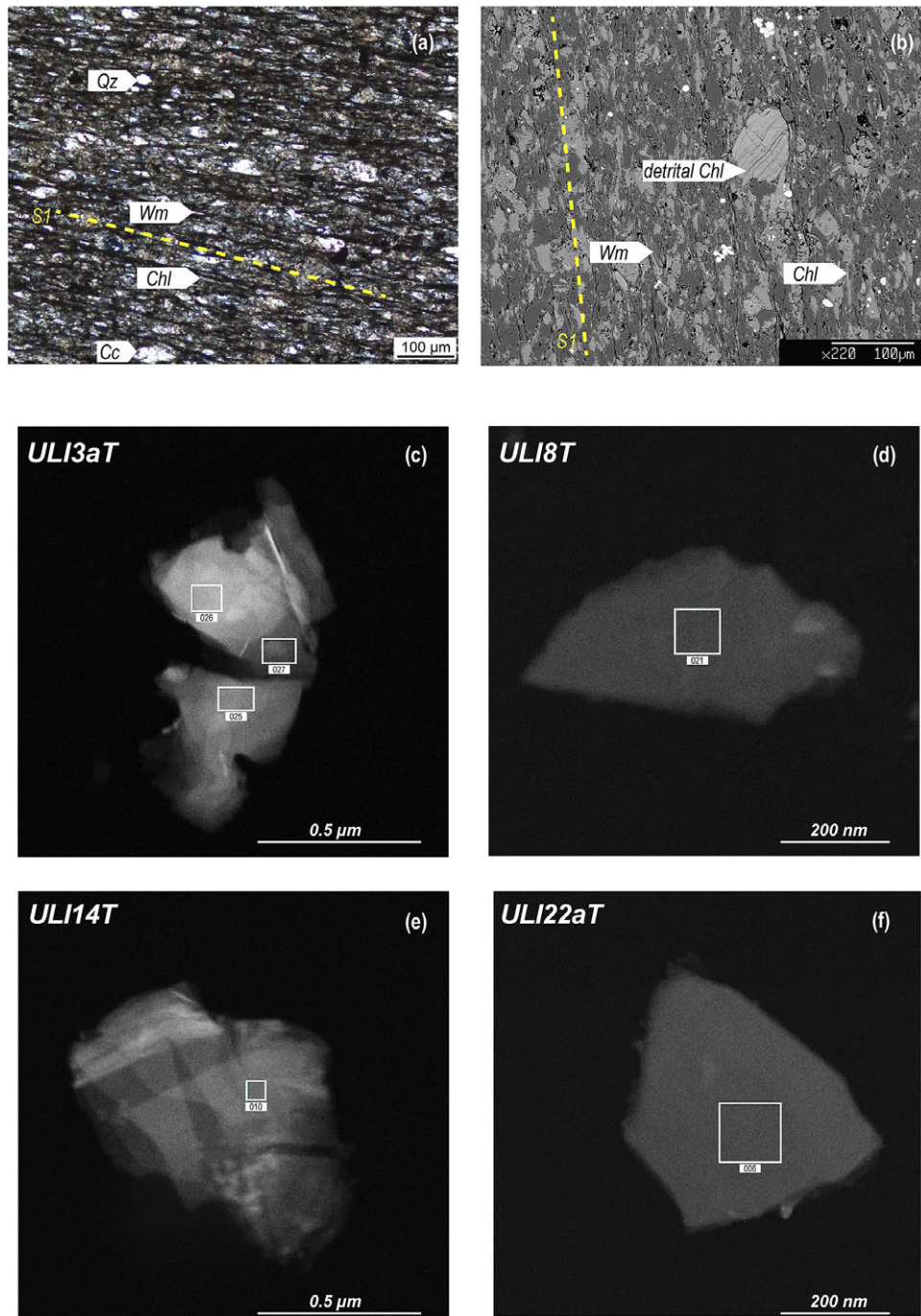


Figure 2. (a) Microtextural features of S1 foliation (dashed yellow line) at the optical microscope. (b) Back-scattered electron image of S1 foliation (dashed yellow line). White mica and chlorite grains are indicated (white arrows). Dark-field TEM images showing representative white mica grains typical for each investigated sample: sample ULI3aT (c); sample ULI8T (d); sample ULI14T (e); and sample ULI22aT (f).

based on the electroneutrality criterion; and (2) the same analyses shown in wt.% of oxides are used for the structural formula recalculations, which can be compared directly with EPMA results, avoiding any error propagation or rounding effect.

k-factor measurement

The database of the JEOL Analysis Station software includes a list of *k*-factors for all elements based on factory standards (see Table 1). These *k*-factors are generally assumed appropriate for all kinds of

samples. However, it has been demonstrated that TEM-EDS analyses improve strongly when a suite of *k*-factors is calculated on standards related structurally and chemically to the sample of interest (e.g. Bourdelle *et al.*, 2012; Conconi *et al.*, 2023). To evaluate the impact of the *k*-factors, a new suite of 13 experimentally derived *k*-factors was extrapolated using 14 minerals and two synthetic compounds (reference materials used as standards are reported in the Supplementary material SI-S4). The reference materials are the same as used by Conconi *et al.* (2023) and their chemical compositions had been checked with EPMA.

Table 1. List of the extrapolated and theoretical *k*-factors used in this paper

Element	Experimentally derived <i>k</i> -factors	<i>k</i> -factors factory
Si	1.00*	1.00*
Ti	1.49	1.34
Al	1.01	0.49
Cr	1.66	1.46
Fe	1.64	1.63
Mn	1.50	1.56
Mg	1.00	0.96
Ca	1.21	1.20
Na	1.04	1.15
K	1.16	1.13
O	0.90**	1.78

*Reference

**average between k_O of biotite and muscovite.

Because these *k*-factors were calculated to be used with the absorption correction method, they were derived from spot analyses collected at various thicknesses in the samples and then extrapolated to 0-thickness (such extrapolated *k*-factor values are reported in Table 1), as reported in Conconi et al. (2023). It is evident that extrapolated *k*-factors for the same element, but obtained from various mineralogical species, are somehow different. In addition, *k*-factor values differ slightly from those calculated by Conconi et al. (2023), as expected for a different instrument and different experimental settings. However, the overall trend is consistent with theoretical expectations: *k*-factor values tend to increase if the atomic number decreases or increases with respect to Si, which is generally used as the reference element ($k=1$).

Remarkably, all cationic species (e.g. Al, K, Na, Ca) show *k*-factor values significantly less scattered than oxygen. According to Conconi et al. (2023), this effect is the consequence of the low energy of $O_{K\alpha}$ radiation, which is easily absorbed with different magnitudes by minerals with different structures and densities. This observation suggests use of a *k*-factor for oxygen (k_O) based only on those minerals that are structurally and chemically close to the specific mineral to be investigated (Wm in this paper). Indeed, k_O obtained for the only two phyllosilicate standards used in the calibration, biotite and muscovite, were roughly similar: 0.82 and 0.98, respectively. In this study, a k_O that is the average of these two values, i.e. 0.90, is used. This k_O is assumed to be a rather good estimation for TEM-EDS measurements of any type of phyllosilicates. In the Supplementary material SI-S5, corrected chemical analyses of Chl grains are also provided. These preliminary analyses were performed using the same k_O chosen for the Wm and the obtained results corroborate the criteria adopted for k_O determination.

By contrast, for all cations, the *k*-factors corresponding to the average values obtained from all standards were used. When consistent, a larger suite of measured standards evidently increases the robustness of the determined *k*-factors.

Data reduction methods

The STL, NC, and ACM methods are applied in this paper to quantify TEM-EDS analyses from metamorphic Wm crystals and

to compare the results with the EPMA values obtained previously. A brief description of the three methods used is reported as follows:

- (i) STL data reduction is already implemented in the JEOL Analysis Station software in the option 'Ratio', in order to obtain non-calibrated chemical analyses with theoretical *k*-factors (see Supplementary material SI-S1). No corrections are applied.
- (ii) In the NC data reduction, no correction for absorption is applied, but experimentally derived *k*-factors measured on standards of known composition and extrapolated for thickness = 0 are used, following the procedure proposed by Conconi et al. (2023).
- (iii) In ACM data reduction, experimentally derived *k*-factors measured on standards of known composition and extrapolated for thickness = 0 are used and a correction for absorption based on the thickness calculated by the electroneutrality criterion (Conconi et al. 2023) is applied.

Absorption correction is usually applied when dense and/or thick specimens are investigated. The main problem related to absorption correction is the difficulty of determining the sample thickness for each spot analysis. Various approaches have been proposed to calculate experimentally the sample thickness (these are summarized in Watanabe et al., 1996; Williams and Carter, 1996; Watanabe and Williams 2006), but none is of practical use when a large number of analyses has to be managed. Besides, many of these approaches need to monitor the beam current value carefully. Conversely, van Cappellen and Doukhan (1994) proposed an absorption correction method based on electroneutrality, in which experimental measurements of beam current and thickness are not required.

When the ACM based on electroneutrality is used, special attention must be paid to hydrated minerals. Indeed, because hydrogen is not detected by WDS and EDS, mineral compositions are commonly recalculated on the basis of completely anhydrous negative charges. For instance, the structural formula of Wm, $(K, Na)(Al, Mg, Fe, Mn)_2(Si, Al)_4O_{10}(OH)_2$, is recalculated on the basis of 11 anhydrous oxygen, instead of 12. Although this method does not alter the measured cation proportions, when used for the TEM-EDS absorption correction it may lead to physically unreliable negative values of thicknesses calculated through the electroneutrality criterion. To overcome this problem, in the calculation of the thickness through electroneutrality we used a reduced oxygen valence, taking into account the contribution of hydrogen. In this way, considering a total of 22 negative charges, $10 O^{2-} + 2 OH^-$, and not considering fluoride and chloride anions, in Wm the net valence of each oxygen is $1.83 e^-$ ($22 e^-/12$). For comparison, in chlorite, $(Mg, Fe)_3(Si, Al)_2O_5(OH)_4$, with 14 negative charges and 9 oxygen atoms, the net valence of each oxygen is $1.56 e^-$. However, once corrected for absorption, the mineral formula must be recalculated on an integral basis of anhydrous oxygen (12 for Wm) for comparison with EPMA and geobarometric applications.

Note that the Cr content was always considered during the charge balance check. However, because of the very small amount (maximum 0.01–0.02 atoms per formula unit, a.p.f.u.), Cr was not included in the final recalculated formula used for the comparison with (already published) EPMA chemical analyses, in which Cr_2O_3 wt.% was considered negligible.

EPMA data acquisition

All EPMA chemical analyses of Wm used in this study have already been published in previous works (ULI14, Meneghini et al., 2023;

ULI3a, ULI8, ULI22a, Sanità *et al.*, 2024). In these papers, the same EPMA apparatus JXA 8200 was used to perform the chemical analyses, either at the Department of Earth Sciences 'A. Desio' (University of Milano) or at the Institute of Geological Science of Geneva. Both sets of EPMA apparatus are equipped with five wavelength dispersive spectrometers and calibrated with the following standards: wollastonite (Ca, Si), orthoclase (K), albite (Al), periclase (Mg), rhodonite (Mn), TiO₂ (Ti), Al₂O₃ (Al), Fe₂O₃ (Fe), and Cr₂O₃ (Cr). The acquisition conditions were 15 keV accelerating voltage, 17 nA sample current, and 20 ms per grid point counting time. A total of 10 spot analyses per sample were collected (see [Supplementary material SI-S6](#)).

Results

For each powdered sample, ~30 chemical analyses were collected from various grains of Wm using spot analysis mode performed on a small squared area of about 50×50 nm. Examples of some investigated grains

are reported in [Fig. 2c–f](#). Only grains showing sizes ranging between 0.5 and 1.0 μm were considered. All chemical analyses are reported in the [Supplementary material SI-S1, -S2, and -S3](#).

As explained in the previous section, EDS data were elaborated following three different procedures: (i) STL with theoretical *k*-factors; (ii) NC with experimentally derived *k*-factors and no absorption correction; and (iii) ACM with experimentally derived *k*-factors for a thickness estimated using the electroneutrality criterion. For the latter group, only those analyses where the electroneutrality was achieved with a deviation within ±0.04 e⁻ were considered as reliable. Regardless of the analytical procedure adopted, all analyses that fell out of 95% (2σ) confidence for SiO₂, TiO₂, Al₂O₃, FeO, MnO, MgO, Cr₂O₃, CaO, Na₂O, or K₂O were omitted. The final output corresponds to 10–20 chemical spot analyses for each sample, for a total of 71, 63, and 64 analyses using STL, NC and the ACM, respectively.

[Figures 3, 4, and 5](#) show the plots of cation contents for each data-reduction procedure. Only the plots of the six major elements

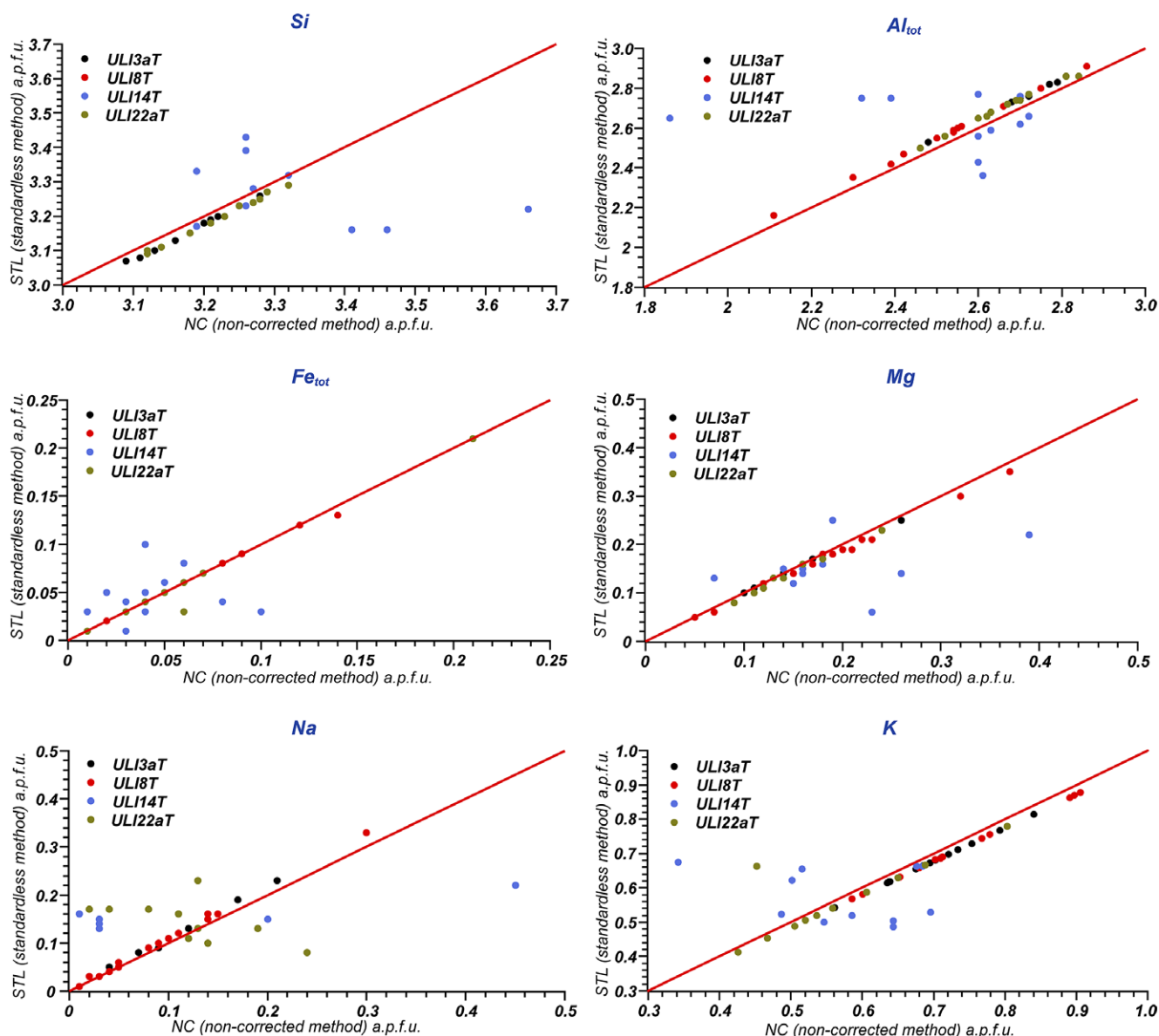


Figure 3. STL (standardless method) vs NC (non-corrected method) data-reduction plots for the TEM-EDS analyses. Only the cations showing significant variations are reported. The red lines indicate a 1:1 ratio between the quantification performed with the two data reductions.

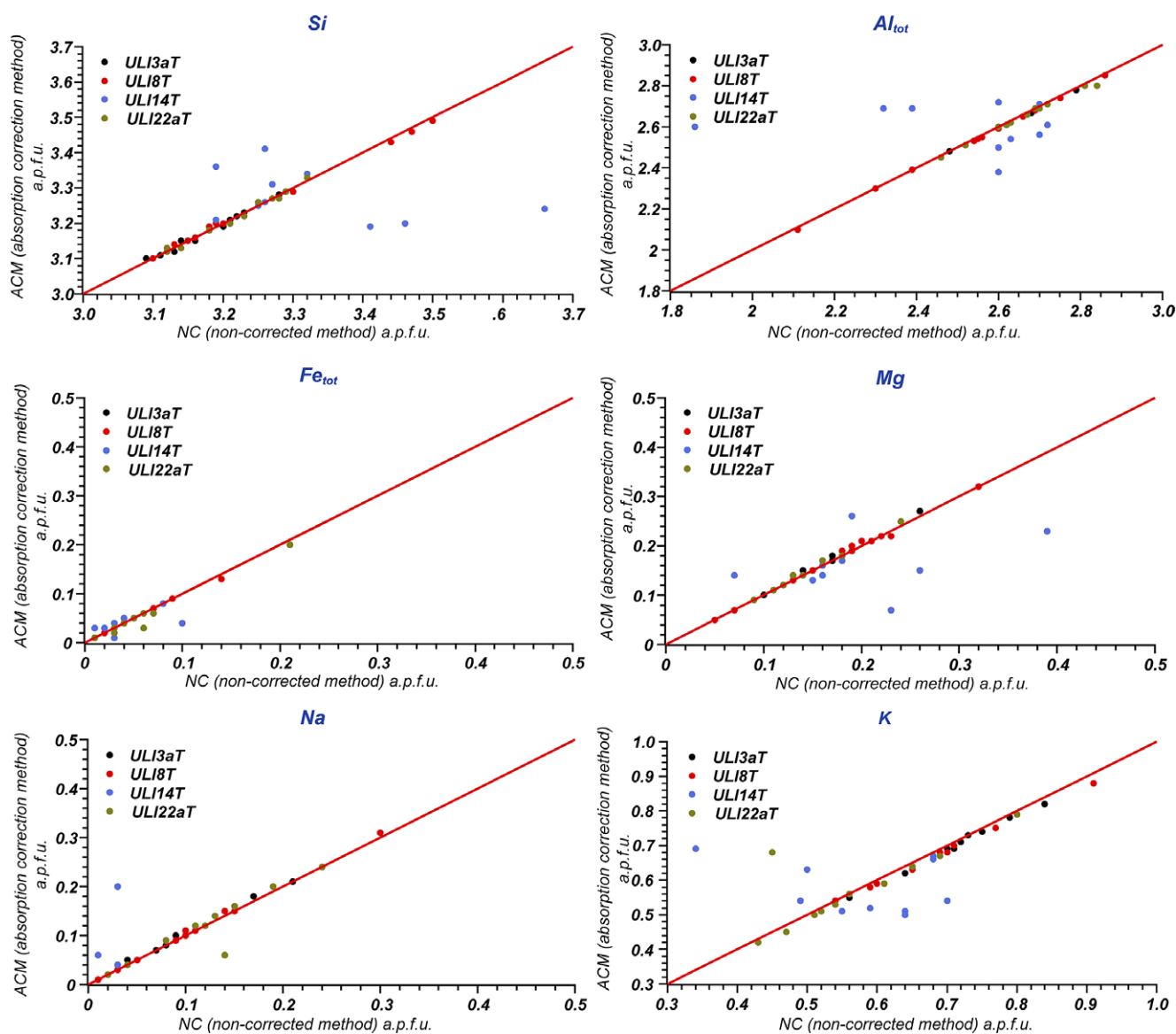


Figure 4. NC (non-corrected method) vs ACM (absorption correction method) plots for the TEM-EDS analyses. Only the cations showing significant variations are reported. The red lines indicate a 1:1 ratio between the quantification performed with the two data reductions.

are reported. Overall, sample ULI14T presents the most scattered values for all cations considered, regardless of which reduction procedure was applied (see Figs 3–5), with the most significant dispersions for K-, Mg- and Fe_{tot}- and Na-contents.

The plots highlight a shift for Si- and Al_{tot}-contents when STL data reduction is used. The shift towards the left side of the 1:1 line for the Si-content (red in Figs 3–5) is systematically counterbalanced by a shift towards the right side for the Al_{tot}-content. These correlated shifts fall within a range of ± 0.05 a.p.f.u. from the 1:1 line and are evidently associated with the different absolute values of STL *k*-factors for Al compared with NC *k*-factors.

In Table 2, the average values and the related standard deviations are reported for each cation, grouped according to the applied reduction method. The interlayer (A-site) and octahedral (M-site) cation sums are also reported (average values and standard deviations). The highest standard deviations are always associated with the STL data reduction: ± 0.19 a.p.f.u. for Al_{tot}-content and ± 0.12 a.p.f.u. for Si-content in

ULI8T and ± 0.11 a.p.f.u. for K-content in ULI22aT. Concerning the cation sums, the highest standard deviations are generally observed for the A-site (± 0.10 a.p.f.u.). Only the sample ULI8T shows a greater scatter for the M-site (± 0.06 a.p.f.u.).

When the NC data reduction is used, no significant change occurs in terms of standard deviations, except for sample ULI14T. In this case, the results are characterized by larger standard deviation values (up to ± 0.13 a.p.f.u. for Al; see Table 2).

Instead, if the ACM is applied, the standard deviations for each single cation, as well as the standard deviations for A- and M-site sums, tend to reduce values. This result implies a significant improvement in data precision and robustness (see Table 2). Besides, the average values for the octahedral sum decrease progressively from data reduction by STL to data reduction by NC and ACM, reaching in this latter case the more feasible value of < 2.10 a.p.f.u. This is a good indicator that the quality of results has improved (see the discussion on Abad et al., 2006). Remarkably, the reduction of cation sums in the octahedra is also observed for the most problematic sample ULI14T.

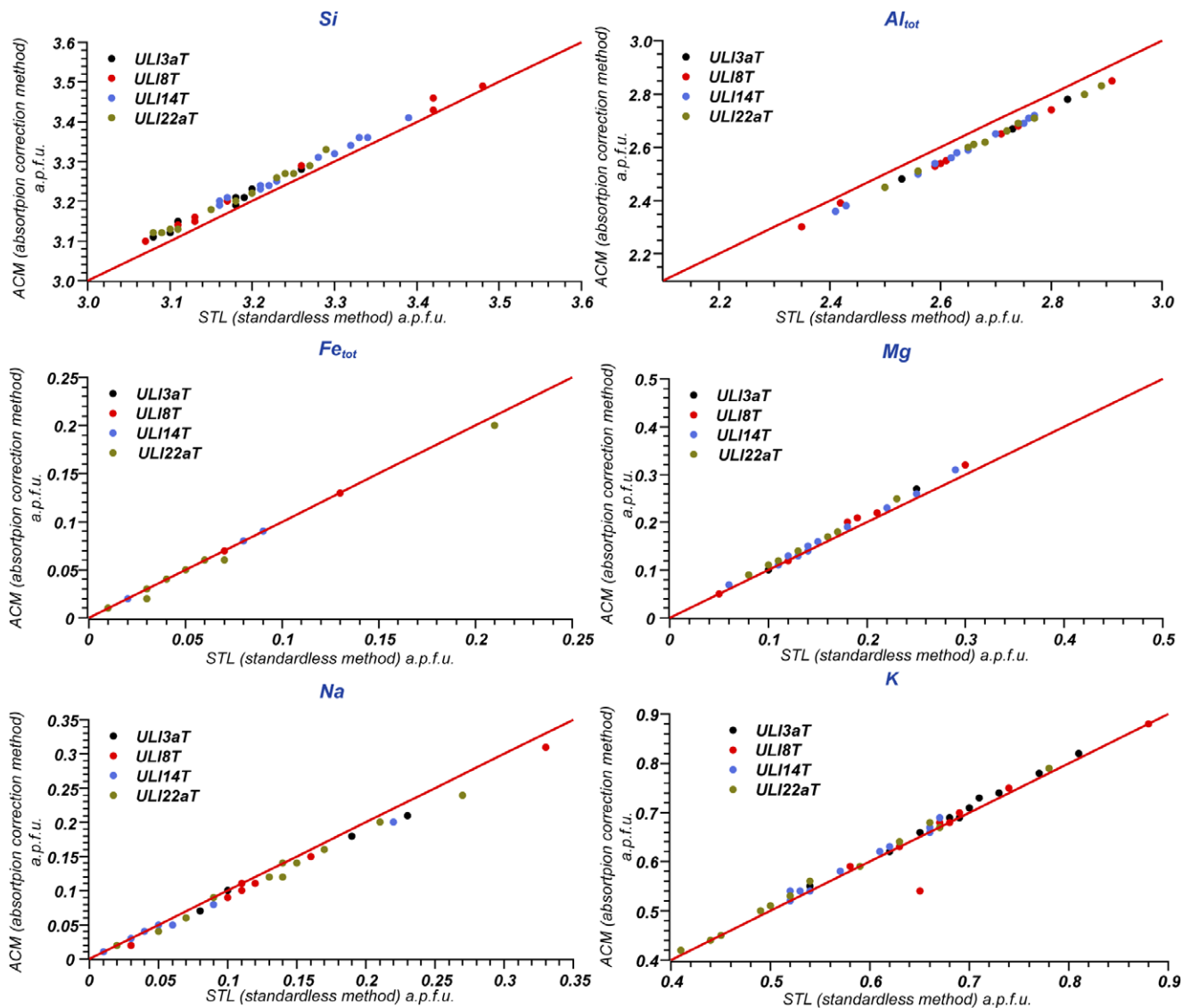


Figure 5. ACM (absorption correction method) vs STL (standardless method) data-reduction plots for the TEM-EDS analyses. Only the cations showing significant variations are reported. The red lines indicate a 1:1 ratio between the quantification performed with the two data reductions.

Table 2. Mean values and related standard deviations of cations are reported for all the data-reduction procedures considered in this paper

		Si (a.p.f.u.)	Al _{tot} (a.p.f.u.)	Fe _{tot} (a.p.f.u.)	Mg (a.p.f.u.)	Na (a.p.f.u.)	K (a.p.f.u.)	T-site (a.p.f.u.)	M-site (a.p.f.u.)	A-site (a.p.f.u.)
STL	ULI3aT	3.15±0.05	2.74±0.09	0.02±0.01	0.15±0.04	0.10±0.05	0.68±0.07	4.00±0.00	2.07±0.03	0.79±0.07
	ULI8T	3.22±0.12	2.60±0.19	0.06±0.04	0.18±0.08	0.10±0.08	0.70±0.10	4.00±0.00	2.06±0.06	0.82±0.10
	ULI14T	3.26±0.08	2.64±0.12	0.05±0.02	0.15±0.05	0.03±0.03	0.57±0.07	4.00±0.00	2.11±0.03	0.62±0.07
	ULI22aT	3.18±0.07	2.72±0.12	0.06±0.05	0.13±0.06	0.05±0.03	0.56±0.10	4.00±0.00	2.12±0.04	0.69±0.07
NC	ULI3aT	3.18±0.05	2.70±0.09	0.02±0.01	0.16±0.04	0.09±0.05	0.70±0.07	4.00±0.00	2.06±0.03	0.80±0.07
	ULI8T	3.25±0.13	2.59±0.02	0.06±0.04	0.18±0.08	0.09±0.07	0.72±0.11	4.00±0.00	2.05±0.06	0.82±0.11
	ULI14T	3.32±0.14	2.52±0.25	0.04±0.03	0.19±0.08	0.02±0.02	0.57±0.11	4.00±0.00	2.09±0.05	0.65±0.10
	ULI22aT	3.22±0.07	2.44±0.11	0.06±0.05	0.14±0.06	0.05±0.03	0.56±0.11	4.00±0.00	2.11±0.04	0.68±0.10
ACM	ULI3aT	3.18±0.05	2.69±0.09	0.02±0.01	0.16±0.04	0.08±0.04	0.69±0.07	4.00±0.00	2.06±0.03	0.79±0.07
	ULI8T	3.23±0.12	2.58±0.21	0.05±0.04	0.19±0.07	0.08±0.05	0.69±0.07	4.00±0.00	2.07±0.02	0.77±0.07
	ULI14T	3.28±0.06	2.60±0.11	0.04±0.02	0.16±0.06	0.03±0.02	0.58±0.07	4.00±0.00	2.09±0.01	0.62±0.07
	ULI22aT	3.21±0.08	2.66±0.12	0.06±0.05	0.14±0.06	0.12±0.06	0.56±0.11	4.00±0.00	2.08±0.04	0.69±0.08

T = tetrahedral sum; M = octahedral sum; A = interlayer sum.

Discussion

Reliability of the data-reduction procedures

Three different methods for chemical data reduction were applied to TEM-EDS analyses of Wm. A first observation concerns the use of appropriate standards before TEM-EDS experiments. A comparison analysis performed between STL and NC methods shows significant and opposite shifts of equal magnitude between Si- and Al_{tot} contents (Fig. 3), regardless of whether the absorption correction is applied or not.

Moreover, the application of ACM led to a significant improvement in data quality, from both a statistical and a crystallo chemical point of view. This effect was particularly evident for sample ULI14T, where a larger scattering of values was initially observed (Fig. 5). A comparison between average chemical analyses obtained using the NC and ACM data reductions highlighted that there is no significant difference. However, if the ACM is applied, the cation contents and the interlayer and octahedral sums are characterized by lower standard deviations.

Comparison with EPMA

Because the ACM data reduction yielded the most satisfying results, only data related to this procedure were compared with EPMA data. As for TEM-EDS, all EPMA analyses that fell out of 95% (2σ) confidence for SiO₂, TiO₂, Al₂O₃, FeO, MnO, MgO, CaO, Na₂O, or K₂O were discarded. In Table 3, EPMA chemical analyses obtained from the investigated samples are reported. Only the average values with the related standard deviations are shown (see Supplementary material SI-S6 for oxide wt.%).

Overall, EPMA and TEM-EDS are characterized by cation contents with comparable standard deviations (cf. Tables 2 and 3). This is already a remarkable result, as TEM-EDS data can be collected from far smaller grains and sample areas. Moreover, looking in greater detail, at least for three samples (ULI3aT, ULI14T, and ULI22aT), values from TEM-EDS are even less scattered than values from EPMA. For ULI14T, the Al content is characterized by the most significant difference with EPMA data, where standard deviations are up to 0.07 a.p.f.u. greater than in TEM-EDS data. For ULI22T, TEM-EDS Si-, Al-, and Fe_{tot} contents are characterized by smaller standard deviations (up to 0.23 a.p.f.u. for Fe_{tot}). Only the

Na- and K contents are characterized by slightly greater scattering values (0.01 a.p.f.u.) than for EPMA. For sample ULI3aT only the interlayer cations and their sum are characterized by slightly greater standard deviations (up to 0.02 a.p.f.u.) for TEM-EDS data. By contrast, Si-, Fe_{tot}-, Mg-, Al contents and the octahedral sum values obtained by TEM-EDS were less scattered, with differences in standard deviations up to 0.07 a.p.f.u..

For sample ULI8, EPMA analyses have greater standard deviations compared with TEM-EDS for Fe_{tot} content and octahedral sum, with differences of 0.04 and 0.03 a.p.f.u., respectively. By contrast, EPMA analyses for Si-, Mg-, Al-, Na-, and K-contents and the A-site sum show less dispersed values than TEM-EDS.

Also, the comparison of the crystal chemistry obtained by TEM-EDS and that determined by EPMA yielded interesting information. In Fig. 6, the Si-Al_{tot} plot and Si-K diagram for EPMA and TEM-EDS analyses are reported. In the Si-Al_{tot} diagram, the red line marks the Tschermak substitution and the solid solution between muscovite-celadonite end members (Fig. 6a). Both EPMA and TEM-EDS analyses strongly indicate that the investigated white mica grains can be represented by a celadonite-muscovite solid solution. Moreover, regardless of the data-reduction method, the samples ULI3aT and ULI22aT are characterized by muscovite-rich compositions, whereas a higher celadonite content for ULI14T and ULI8T is observed. These findings are supported by the Si-K plot (Fig. 6b). Both EPMA and TEM-EDS yielded values of ~0.50–0.88 and 3.10–3.48 a.p.f.u. of K and Si, respectively. This is a good fit, taking into account that an accurate analysis of weakly bonded interlayer cations in phyllosilicates, such as K and Na, may be problematic due to diffusion under the highly focused TEM electron beam. Moreover, for sample ULI22aT, both EPMA and TEM-EDS analyses yielded controversial results, with K and Si contents <0.50 and <3.00 a.p.f.u., respectively. This effect is probably associated with some undisclosed sample features and does not depend on the analytical procedure adopted.

Summarizing, the comparison between TEM-EDS chemical analyses, quantified with the ACM and EPMA data yielded satisfactory results supporting the reliability of the data-reduction procedure described in this paper. The protocol was successful in terms of delivering TEM-EDS analyses that corroborate from a chemical and statistical point of view those obtained by EPMA.

Table 3. EPMA analysis of the same samples analyzed by TEM-EDS

	ULI3b* (a.p.f.u.)	ULI8* (a.p.f.u.)	ULI14** (a.p.f.u.)	ULI22a* (a.p.f.u.)
Si	3.11±0.06	3.21±0.07	3.15±0.09	3.13±0.14
Al _{tot}	2.75±0.10	2.47±0.03	2.69±0.18	2.49±0.17
Fe _{tot}	0.12±0.08	0.16±0.08	0.09±0.04	0.36±0.28
Mg	0.09±0.05	0.19±0.05	0.11±0.07	0.22±0.11
Na	0.12±0.02	0.05±0.01	0.09±0.05	0.12±0.04
K	0.74±0.05	0.75±0.03	0.76±0.08	0.52±0.10
T-site	4.00±0.00	4.00±0.00	4.00±0.00	4.00±0.00
M-site	2.07±0.06	2.09±0.07	2.06±0.03	2.24±0.19
A-site	0.86±0.05	0.80±0.03	0.86±0.07	0.64±0.09

Only the average and the related standard deviations are reported.

*Data from Sanità et al. (2024)

**Data from Meneghini et al. (2023).

Summary of the strategy adopted and conclusions

The results of this work indicate that the strategy adopted, including sample preparation and data reduction based on the electroneutrality criterion, can guarantee high-quality chemical data on fine-grained hydrous phyllosilicates. Such a strategy is characterized by advantages and disadvantages which are detailed as follows.

Advantages

Our protocol could be used to investigate sub-micrometer sized materials, following the powdered samples procedure. This preparation enables a Wm-rich powder to be investigated by the TEM-EDS apparatus using a low-cost treatment, if compared with the FIB and/or ion mill techniques, with no evidence of chemical or physical damage.

ACM data reduction yielded satisfactory results, improving the quality and the accuracy of chemical analyses of phyllosilicates. The use of experimentally derived *k*-factors gave much more reliable

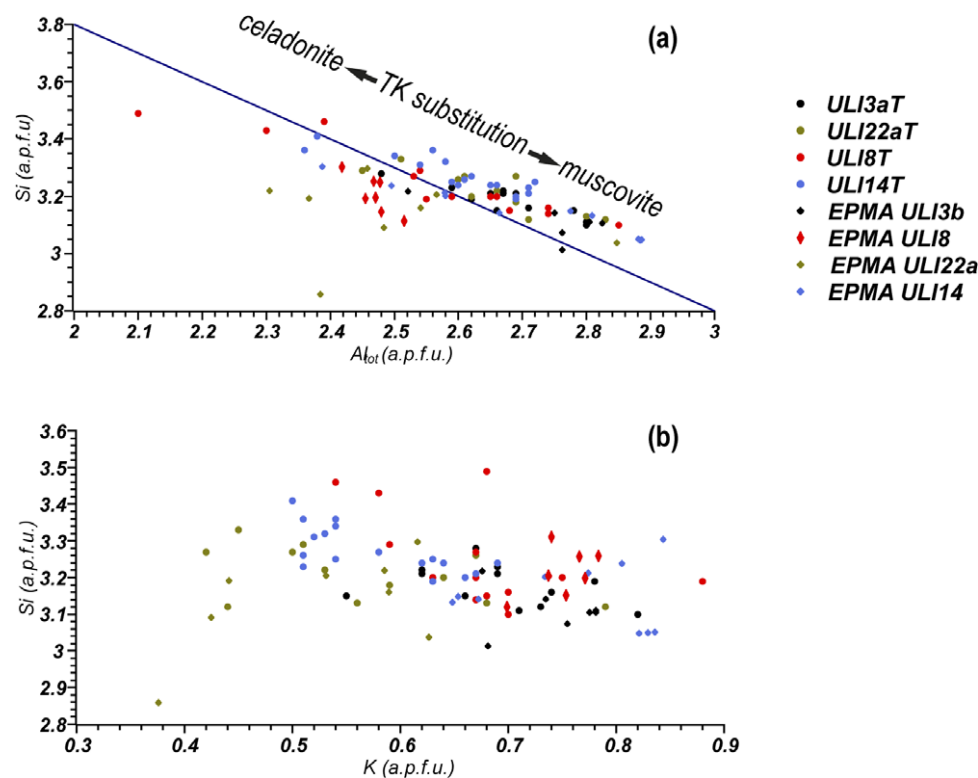


Figure 6. (a) Si- Al_{tot} and (b) Si-K diagrams for EPMA and TEM-EDS (after ACM) analyses. The blue line in (a) indicates the celadonite—muscovite solid solution with Tschermak (TK) substitution.

results compared with factory-implemented k -factors, representing the first crucial step to get values with accuracies comparable with an EPMA apparatus. The most controversial point concerns the determination of the k -factor for oxygen (k_O). The scattering observed for k_O suggested that this value is strongly related to the structure and the density of the material, and therefore it is recommended to select only standards close to the actual target of the TEM-EDS analyses. It is worth pointing out that oxygen accounts for almost the whole anion curve used for thickness estimation (see Conconi *et al.*, 2023), and an incorrect calibration of k_O will unavoidably lead to incorrect chemical outputs. Another critical point concerns the inclusion of hydrogen in the calculation for electroneutrality, which appeared critical for the investigation of Wm, and even more for the preliminary tests on chlorites (see Supplementary material SI-S5).

Overall, the protocol illustrated in this work for recalculating structural formulae gave acceptable standard deviations, not substantially different from those determined by EPMA. This procedure could find applications for the refinement of already calibrated geothermobarometers, improving the ability to estimate pressure and temperature conditions of metamorphic rocks characterized by very fine-grained mineral assemblages.

Disadvantages

The obvious disadvantage of this sample preparation is that the rock micro-texture is not preserved. Besides, the application of ACM led to the rejection of several chemical analyses. However, if an appropriate amount of spot analyses is performed, a reasonable number of statistically sound and highly accurate chemical analyses can be achieved easily.

Based on the above considerations, the following analytical protocol is proposed for enhancing the probability of good chemical analyses of microcrystalline geologic samples:

- Sample preparation must be carried out on rock samples in which the mineral phase (or the mineral phases) of interest is present in large amounts. A detailed petrographic investigation with optical and electron microscopy is recommended to check the size of the material of interest.
- Experimental k -factors must be extrapolated using standards of known compositions, paying particular attention to the oxygen k -factor value. k_O should be determined taking into account the mineral phase selected for the investigation (e.g. phyllosilicates, tectosilicates, oxides, carbonates). The extrapolation of new k -factors is recommended regardless of the type of instrument used to perform the analysis. The extrapolated k -factors for this work are slightly different from those calculated by Conconi *et al.* (2023). Consequently, for each TEM-EDS device a unique suite of k -factors is expected.
- ACM data reduction, as described above, must be performed to obtain high-quality chemical compositions with smaller values for standard deviation.

To date, the EPMA remains the most established device to determine high-quality chemical data for major and minor elements. However, its application is not recommended if the investigated materials have a grain size of $<5 \mu\text{m}$, because there is a significant risk of obtaining contaminated chemical compositions. The procedure described in this work pushes further the crystal size limit, in order to perform reliable chemical analyses on grains which are smaller than $1 \mu\text{m}$, like the Wm in low-grade metapelites.

Supplementary material. The supplementary material for this article can be found at <http://doi.org/10.1017/cmn.2024.32>.

Author contribution. Conceptualization: E.S., E.M.; Methodology: E.S., R.C., S.L.; Software: E.S., R.C., S.L.; Validation: E.S., R.C., M.D.R., G.C., E.M.; Formal analysis: E.S., R.C.; Investigation: E.S., R.C.; Resources: E.S., E.M.; Data curation: E.S., R.C.; Writing - original draft: E.S.; Writing - review & editing: E.S., R.C., S.L., G.C., M.D.R., E.M.; Visualization: E.S., R.C.; Supervision: E.S., E.M.; Project administration: E.S., E.M.

Acknowledgements. Michele Marroni and Luca Pandolfi are thanked for making available the samples investigated in this work. A special thanks to Michele Alderighi for his technical support during the TEM-EDS data acquisition. The authors thank the Centre for Instrument Sharing of the University of Pisa (CISUP) for the use of TEM-EDX apparatus. The Editor-in-Chief, the Associate Editor and two anonymous reviewers are also thanked for constructive and stimulating comments and suggestions that improved the final version of the manuscript.

Financial support. This work was funded by PRIN Project 2020 (awarded to Michele Marroni).

Competing interests. The authors declare no competing interests.

Data availability statement. Data are available from the authors on request.

References

- Abad, I., Nieto, F., Gutiérrez-Alonso, G., Campo, M.D., López-Munguira, A., & Velilla, N. (2006). Illitic substitution in micas of very low-grade metamorphic clastic rocks. *European Journal of Mineralogy*, 18, 59–69.
- Battaglia, S. (2004). Variations in the chemical composition of illite from five geothermal fields: a possible geothermometer. *Clay Minerals*, 39, 501–510.
- Benzerara, K., Menguy, N., Guyot, F., Vanni, C., & Gillet, P. (2005). TEM study of a silicate–carbonate–microbe interface prepared by focused ion beam milling. *Geochimica et Cosmochimica Acta*, 69, 1413–1422.
- Bourdelle, F., Parra, T., Beyssac, O., Chopin, C., & Moreau, F. (2012). Ultrathin section preparation of phyllosilicates by focused ion beam milling for quantitative analysis by TEM-EDX. *Applied Clay Science*, 59, 121–130.
- Cliff, G., & Lorimer, W. (1975). The quantitative analysis of thin specimens. *Journal of Microscopy*, 103, 203–207. <https://doi.org/10.1111/j.1365-2818.1975.tb03895.x>.
- Conconi, R., Ventruti, G., Nieto, F., & Capitani, G. (2023). TEM-EDS microanalysis: comparison among the standardless, Cliff & Lorimer and absorption correction quantification methods. *Ultramicroscopy*, 254, 113845.
- Dubacq, B., Vidal, O., & De Andrade, V. (2010). Dehydration of dioctahedral aluminous phyllosilicates: thermodynamic modelling and implications for thermobarometric estimates. *Contribution to Mineralogy and Petrology*, 159, 159–174.
- Guidotti, C.V., & Sassi, F.P. (1998). Petrogenetic significance of Na-K white mica mineralogy: recent advances for metamorphic rocks. *European Journal of Mineralogy*, 10, 815–854.
- Kamzolkin, V.A., Ivanov, S.D., & Konilov, A.N. (2016). Empirical phengite geobarometer: Background, calibration, and application. *Geology of Ore Deposits*, 58, 613–622.
- Kübler, B. (1967). La cristallinité de l'illite et les zones tout à fait supérieures du métamorphisme. In *Etages Tectoniques, Colloque de Neuchâtel 1966*, pp. 105–121. Université Neuchâtel, à la Baconnière, Suisse.
- Lezzerini, M., Sartori, F., & Tamponi, M. (1995). Effect of amount of material used on sedimentation slides in the control of illite 'crystallinity' measurements. *European Journal of Mineralogy*, 7, 819–823.
- Leoni, L., Marroni, M., Sartori, F., & Tamponi, M. (1996). Metamorphic grade in metapelites of the internal liguride units (Northern Apennines, Italy). *European Journal of Mineralogy*, 8, 35–50.
- Marroni, M., & Pandolfi, L. (1996). The deformation history of an accreted ophiolite sequence: the Internal Liguride units (Northern Apennines, Italy). *Geodinamica Acta*, 9(1), 13–29.
- Marroni, M., Meneghini, F., & Pandolfi, L. (2010). Anatomy of the Ligure-Piemontese subduction system: evidence from Late Cretaceous–middle Eocene convergent margin deposits in the Northern Apennines, Italy. *International Geology Review*, 52, 1160–1192.
- Marroni, M., Meneghini, F., & Pandolfi, L. (2017). A revised subduction inception model to explain the Late Cretaceous, double-vergent orogen in the pre-collisional western Tethys: evidence from the Northern Apennines. *Tectonics*, 36, 2227–2249.
- Massone, H.J., & Schreyer, W. (1987). Phengite barometry based on the limiting assemblage with K-feldspar, phlogopite and quartz. *Contributions to Mineralogy and Petrology*, 96, 212–224.
- Meneghini, F., Di Rosa, M., Marroni, M., Raimbourg, H., & Pandolfi, L. (2023). Subduction signature in the Internal Ligurian units (Northern Apennine, Italy): evidence from P–T metamorphic peak estimate. *Terra Nova*, 36, 182–190.
- Newbury, D.E., Swyt, C.R., & Myklebust, R.L. (1995). Standardless quantitative electron probe microanalysis with energy-dispersive X-ray spectrometry: is it worth the risk? *Analytical Chemistry*, 67, 1866–1871.
- Newbury, D.E. (1998). Standardless quantitative electron-excited X-ray microanalysis by energy-dispersive spectrometry: what is its proper role? *Microscopy and Microanalysis*, 4, 585–597. <https://doi.org/10.1017/S1431927698980564>
- Obst, M., Gasser, P., Mavrocordatos, D., & Dittrich, M. (2005). TEM-specimen preparation of cell/mineral interfaces by focused ion beam milling. *American Mineralogist*, 90, 1270–1277.
- Penniston-Dorland, S. C., Bebout, G. E., von Strandmann, P. A. P., Elliott, T., & Sorensen, S. S. (2012). Lithium and its isotopes as tracers of subduction zone fluids and metasomatic processes: Evidence from the Catalina Schist, California, USA. *Geochimica et Cosmochimica Acta*, 77, 530–545.
- Sanità, E., Di Rosa, M., Marroni, M., Meneghini, F., & Pandolfi, L. (2024). Insights into the Subduction of the Ligure-Piemontese Oceanic Basin: new constraints from the metamorphism in the Internal Ligurian Units (Northern Apennines, Italy). *Minerals*, 14, 64.
- Stadelmann, P., Leifer, K., & Verdon, C. (1995). EDS and EELS using a TEM-FEG microscope. *Ultramicroscopy*, 58, 35–41.
- Tarantola, A., Mullis, J., Guillaume, D., Dubessy, J., de Capitani, C., & Abdelmoula, M. (2009). Oxidation of CH₄ to CO₂ and H₂O by chloritization of detrital biotite at 270±5°C in the external part of the Central Alps, Switzerland. *Lithos*, 112, 497–510.
- van Cappellen, E., & Doukhan, J.C. (1994). Quantitative transmission X-ray microanalysis of ionic compounds. *Ultramicroscopy*, 53, 343–349.
- Vidal, O., & Parra, T. (2000). Exhumation paths of high-pressure metapelites obtained from local equilibria for chlorite–phengite assemblages. *Geological Journal*, 35, 139–161.
- Watanabe, M., Horita, Z., & Nemoto, M. (1996). Absorption correction and thickness determination using ζ -factor in quantitative X-ray microanalysis. *Ultramicroscopy*, 65, 187–198. [https://doi.org/10.1016/S0304-3991\(96\)00070-8](https://doi.org/10.1016/S0304-3991(96)00070-8)
- Watanabe, M., & Williams, D.B. (2006). The quantitative analysis of thin specimens: a review of progress from the Cliff-Lorimer to the new zeta-factor methods. *Journal of Microscopy*, 211, 89–109. <https://doi.org/10.1111/j.1365-2818.2006.01549.x>
- Williams, D.B., & Carter, C.B. (1996). *Transmission Electron Microscopy: A Textbook for Materials Science*. Springer US, Boston, MA, USA.
- Warr, L.N. (2021). IMA–CNMNC approved mineral symbols. *Mineralogical Magazine*, 85, 291–320.
- Wirth, R. (2004). Focused ion beam (FIB): a novel technology for advanced application of micro- and nanoanalysis in geosciences and applied mineralogy. *European Journal of Mineralogy*, 16, 863–876.
- Wunderlich, W., Foitzik, A.H., & Heuer, A.H. (1993). On the quantitative EDS analysis of low carbon concentrations in analytical TEM. *Ultramicroscopy*, 49, 220–224.